Journal of Manufacturing Processes 31 (2018) 453–467

Contents lists available at ScienceDirect

Journal of Manufacturing Processes

journal homepage: www.elsevier.com/locate/manpro

Experimental optimization of tab and slot plug welding method suitable for unique lightweight frame structures

Michal Starý[a,*], František Novotný[a], Marcel Horák[a], Marie Stará[b], Zdeněk Vít[b]

[a] Institute for Nanomaterials, Advanced Technologies and Innovation, Technical University of Liberec, Studentská 1402/2, 46117, Liberec 1, Czechia
[b] Faculty of Mechanical Engineering, Technical University of Liberec, Studentská 1402/2, 46117 Liberec 1, Czechia

ARTICLE INFO

Article history:
Received 15 June 2017
Received in revised form
20 November 2017
Accepted 26 November 2017

Keywords:
Tab and slot
Plug weld
Frame
Lightweight structure
Construction system

ABSTRACT

The tab and slot plug welding method applied to frame construction represents an interesting and low-cost construction system. Regarding the materials used, it is possible to create both unique lightweight aluminium frames, applied to service robots or effectors, as well as conventional steel frames for machines and peripherals. This article firstly summarizes the technologies and general aspects of the frame structure, and then it presents the characteristics of the tab and slot plug welding method, followed by a brief theoretical analysis. Furthermore, experimental and numerical simulations are performed based on the comparison of the given method with the common construction system of extruded profiles. The main focus is on optimizing the tab and slot system based on extensive laboratory experiments, where emphasis is placed on the dimensions of the joints in relation to used materials. This is followed by numerical simulation of the stress fields in joints. In the conclusion, recommendations are made for frames of different materials produced by the presented method; Work also includes selected real examples of structural applications of the given system.

1. Introduction to frame design

Frames represent the basic supporting element of most machinery and peripherals, means of transport, but also many buildings. In all cases, the basic criteria are low or acceptable production costs [1] and adherence to proportional design parameters [2]. The most advanced developments in light and ultralight structures can be seen in astronautics [3–5], and subsequently in avionics [6–8] from drones onwards [9,10]. Another important area that develops the application of such technologies and systems for mass use is the automotive industry [11–13]. In all of these areas, the application of lightweight frames has a direct impact on performance, both in terms of performance parameters and cost savings [1,14,15]. However, it is necessary to bear in mind that special structures are often connected with a high purchase price, both in terms of the materials and production technologies used. In standard industrial practice using frame structures, it is necessary to seek a compromise between the cost of production and the resulting parameters of the fabricated structure [16]. Frequent parameters of common structures include, in particular, the requirement for high rigidity, often in relation to lowest possible weight, and, in the case of moving parts, low inertia. Another equally important requirement is the overall level of development of the design task, from both a technical as well as aesthetic point of view.

The development of frame structures generally includes the areas of construction materials, modern methods for dividing and processing the materials and, last but not least, the frame connection technology. These areas are closely intertwined and advancements in one of them often influences and expands the possibilities in other areas. Examples include modern methods of material separation and processing, which provide many new ways of acquiring the desired design [16,17].

Modern cutting technologies include CNC cutting machines based on a laser or water jet, or even plasma, which can favourably reduce costs. This method falls into the promising area of digital fabrication, where the use of metal plates as the input intermediate product enables easy and above all space-saving transport of the resulting fragments to the place of assembly or to the customer. The use of a wide range of plate thicknesses also expands the variability of the resulting assembly. An alternative is the use of 3D printing [9,18,19], which represents an unconventional modern technology in the engineering industry with a wide range of applications, which provides, among other things, a high potential for new types of construction. One of the main advantages is not only

* Corresponding author.
E-mail addresses: michal.stary@tul.cz (M. Starý), frantisek.novotny@tul.cz (F. Novotný), marcel.horak@tul.cz (M. Horák), marie.stara@tul.cz (M. Stará), zdenek.vit@tul.cz (Z. Vít).

https://doi.org/10.1016/j.jmapro.2017.11.029
1526-6125/

the shape variability of the products, but also the possibility to use a wide range of materials and their combinations, from plastics and ceramics to metals.

In general, the most promising materials are composites, which have excellent mechanical properties in relation to low weight. For structural purposes, carbon fibre composites are the most suitable for ultra-light rigid frames [20,21]. However, the purchase price is very high, so in the vast majority of cases they are only used in aviation applications or in luxury cars, etc. Furthermore, the price is also not favourable in terms of production costs, including subsequent machining, because the composites are very hard and abrasive [22,23]. For conventional applications, it is more economical to use conventional materials such as steels, materials based on aluminium alloys, and also titanium or plastics [24–26]. Titanium alloys have the best ratio between maximum strength and minimum weight but their cost is very high and in most cases their use for structural applications would be unprofitable. Conversely, plastics are not widely used as conventional frame structures because of their low rigidity. Steel materials can be divided into conventional and stainless steel in this context. In terms of mechanical properties, conventional structural steels have a relatively high rigidity and a low weight if the rigidity is proportional to the shape relief. The cost of conventional structural steels is relatively low, but the emphasis has to be on the surface treatment. Stainless steels have considerably higher intermediate product costs, which can be partly offset by eliminating surface treatment. Aluminium alloys are best suited for less stressed structures, where emphasis is primarily placed on low weight. Acquisition costs are lower for aluminium alloys than they are for stainless steel, but they are relatively comparable with conventional steel in terms of material density. The products costs depend on the geometrical complexity of the parts in the case of machining, which is closely related to the choice of the machining technology used. By using unconventional cutting methods, the price depends on the dimensional size and usually only marginally from the flat shape complexity.

In addition to the materials and methods of cutting and machining, the formation of non-monolithic frame constructions is closely related to the connection system [27–29], which includes several factors – joining method, locating and holding. Joining can be achieved by adhesion, mechanical components or welding. In the case of the use of mechanical elements, except for self-tapping screws, a hole must be made in both joints to achieve, in addition to the rigid connection, positioning of the part in the correct position relative to the assembly. Positioning can be accomplished by external means, i.e. positioning devices [30], or within the assembly itself, with the help of internal or external (pins) shape elements. Specific positioning devices are particularly suitable for mass production. In the case of single-piece production, universal positioning devices are often used. Positioning systems using external shaped elements in the form of pins or centring cavities etc., carry greater demands on the workpiece, i.e. the production of holes and grooves. In relation to modern cutting technologies, where the complexity of the plate shape is not an essential item in the cost of fabrication, positioning elements may be used as an integral part of the finished product. This is generally referred to as the tab and slot method.

2. Tab and slot method

The tab and slot system is a well-known design system [16,31,32] with a wide range of applications. Perhaps the best known is the use of tabs and slots for the positioning of parts in welded structures (Fig. 1b) [33], thus reducing or even eliminating the requirements for positioning devices. Another structural area utilizing the tab and slot system is the joining of plates, which occurs by means of bending or other deformation of the overhang tabs (Fig. 1d) [34,35]. In a broader sense, a specific manufacturing process called origami [36] can be included in the field. Also, the system is widely used in small workshops, in the construction of frames without welding, where the inserted tabs are deformed in the slot, for example by a punch, or screws are used as fasteners and nuts are inserted into the slot (Fig. 1e).

A less-known yet very promising method is the tab and slot welded construction system, where welding is only performed in the area of the tab and slot joints (Fig. 1c). This is a method with high potential application for producing frames, representing an alternative to conventional welded frames from profiled bars but at similar or even lower production costs. A great advantage of the system is the easy application of relief, while maintaining a comparable or even higher frame rigidity. The main advantage of the tab and slot plug welding system is the shape precision of the resulting welded structure where, unlike the application of continuous or intermittent fillet welds [37–39], there is no thermal deformation of the frame. Another advantage is the ability to create relatively interesting industrial designs of exposed frame structures. By grinding the area of the welds, it is possible to achieve an aesthetically interesting frame without any visible connection. The presented method is able to produce both cheap steel structural frames of equipment and peripheries, as well as lightweight aluminium alloy frames, usable in avionics, effectors and conventional devices requiring a lower weight.

Metal sheets cut by laser, water or plasma cutting centres can be used as intermediate products. The thickness of usable plates is limited, in particular, by the production limits of the cutting centres in relation to the selected material [40–42]. The method is particularly suitable as a replacement for frames of thin-walled profiles, where the thickness of the wall is normally in the range of several millimetres (typically 2 or 3–6 mm). For sheet cutting, any shape relief can be realized, which, when properly designed, results in weight saving of the resulting frame while maintaining its strength and stability. They can also be used for easy access to the internal area of the final frame, for example for electrical wiring, pneumatics or hydraulics.

In order to obtain the optimal strength and appearance parameters of the resulting construction system, including production and cost optimization, it is necessary to observe the basic application procedures. These are mainly given by the optimal shape and dimensions of the tabs and slots, which are dependent on the applied structural material and the thickness of the used plates. To create tabs and slots, there are principles that need to be met for the production technology.

The shape of the tabs and slots is given by the following rules (Fig. 2). In the case of tabs, the width (a) is determined by the thickness of the selected sheet metal. The optimum length of the tabs (b) is assumed in the basic theory of the given technology to be similar to the width, i.e. the base of the tabs is formed by a square or pseudo-square profile, which is derived from the weld plug. Of course, it is also possible to apply a rectangular base profile, which is also the subject of presented optimization, see Chapter 5. The height of the tabs (c) is given by the thickness of the used plate (d) counter piece with the slot, with the specific value being derived from the material used based on the practical knowledge of the local welding technology ($c = f(d)$). The tabs also include recesses to facilitate contact with the surfaces. In addition, the slots must be fitted with characteristic grooves, whose orientation in relation to the mounting must be parallel to the thickness of the opposite plate due to its flatness. The groves are desirable not only in relation to the production technology but also in terms of reducing the local stress in the corners of the elements. The profile of the slot ($g \times h$) is defined by the tab dimensions ($a \times b$), which is increased by approximately 0.2 mm ($g = a + 0.2$ mm, $h = b + 0.2$ mm).

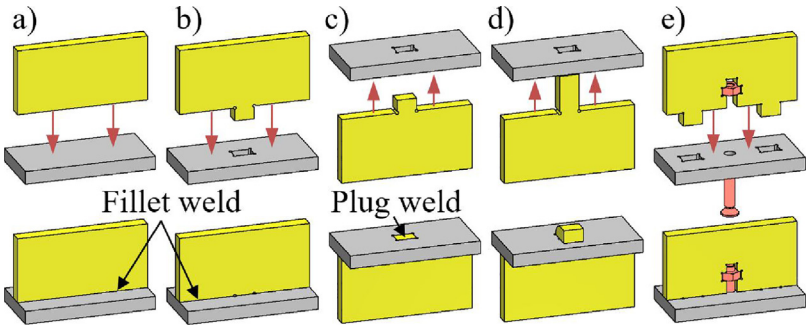

Fig. 1. Installation and connection of basic types of connections – a) Reference joint with fillet weld (requires external fixture), b) Tab and slot butt joint with fillet weld, c) Recessed tab and slot butt joint with plug weld, d) Tab and slot butt joint with bent tab, e) Mechanically fastened butt joint with nut and bolt.

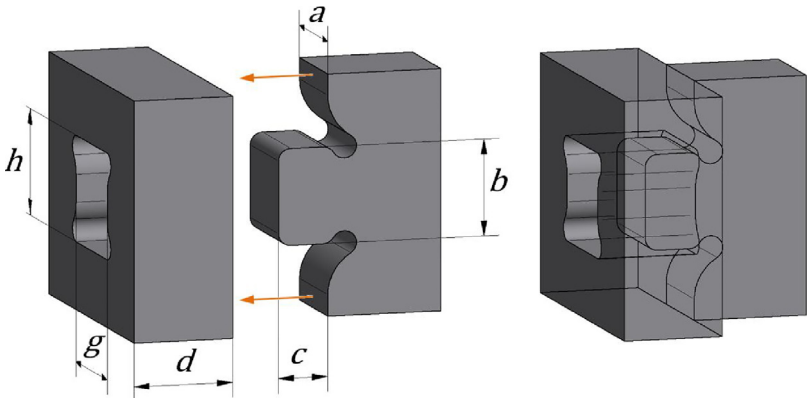

Fig. 2. Dimensional characteristics of the tab and slot system.

The specific value of the addition mainly depends on the accuracy of the cutting machine, which is usually approximately 0.1 mm. In addition to their relation to the shape and position precision of the intermediate product, these are also desirable in view of their easy installation and the possibility of the additional effects of thermal stresses. When welding the joint, the material heats up and the subsequent cooling results in a thermal effect which, due to thermal expansion, produces the desired tightening of the tab and slot connection.

A significant advantage of the tab and slot plug welding method is that the technological process (local welding) results in only minimal thermal deformations of the structure. Due to modern material cutting, the resulting design has fairly accurate dimensional geometry (in the order of tenths of a millimetre) and therefore, in most cases, there is no subsequent complicated and expensive machining of the functional surfaces. Another advantage is the relatively low weight of the resulting structure due to the possibility to apply shape relief while maintaining a sufficiently high rigidity. Last but not least, the tab and slot plug welding systems provide the structure with a high design effect, especially during additional grinding of the local welds, making the final construction look uniform. A design-limiting aspect can be characteristic overhanging of the plates at the edges of the structure, which depend on the thickness of the plate used.

3. Basic theory and calculation

The fixed connection created by the given technology represents a combination of the shape of the fitting and the weld plug or weld slot. The weld is made by the method of fusion welding, which leads to a connection by the local welding of the welding surfaces of the basic materials. The resulting melt pool is further enriched with an additive material of the same or very similar chemical composition as the base material.

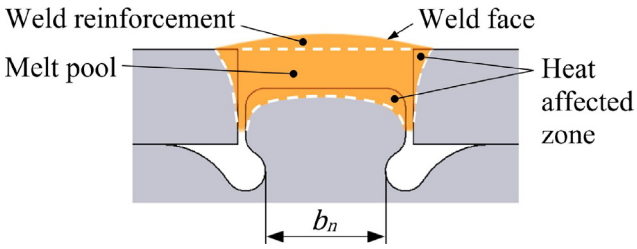

Fig. 3. Cross section of a plug welded joint.

Modelling of the melt pool (Fig. 3) represents a very complex process [43,44], which will be briefly described here. The mathematical equations describing the physical processes taking place within welding processes are those mass and heat flow. The elementary differential equations describe the conservation of mass (1), momentum (2) and energy (3) for an incompressible fluid [45].

$$\nabla \cdot \boldsymbol{u} = 0 \tag{1}$$

$$\rho\left(\frac{\partial \boldsymbol{u}}{\partial t} + \boldsymbol{u}\cdot\nabla\boldsymbol{u}\right) = -\nabla p + \rho\boldsymbol{g} + \mu\boldsymbol{\tau}_{ij} - \boldsymbol{g}\Delta\rho + \boldsymbol{J}x\boldsymbol{B} \tag{2}$$

$$\rho c_p\left(\frac{\partial T}{\delta t} + \boldsymbol{u}\cdot\nabla T\right) = \nabla\cdot(k\nabla T) + \boldsymbol{E} \tag{3}$$

where $\boldsymbol{u}$ is the velocity, ρ is the density, t is the time, $\boldsymbol{g}$ is the gravity, μ is the viscosity, $\boldsymbol{\tau}_{ij}$ is shear stress tensor, p is the pressure, T is the temperature, k is the thermal conductivity, c_p is the specific heat capacity, $\boldsymbol{E}$ is the enthalpy, $\boldsymbol{J}$ is the current density, $\boldsymbol{B}$ is the magnetic flux density. Lorentz force can be solved from Maxwell's equations [45]. A calculation of the flow velocity, pressures and temperatures

requires the simultaneous solution of these Eqs. (1)–(3) under a given or assumed set of boundary conditions. A detailed presentation of these equations and a discussion of the necessary boundary conditions is given by [46].

For a simulation prediction of melting tab and slot welded joints, it would be useful to perform a melt pool analysis to provide information on the course of the molten state and the development of the structure. For the realization of such a task, there are currently only very limited approximate mixed methods in the form of a simple intuitive analysis in the weld bead and FE analysis in the rest of the structure [47]. Comsol Multiphysics [48], Fluent [49] or Flow-3D [50] software is often used for the given task. In general, the application of numerical welding simulations is particularly useful when the aim is to evaluate residual stresses in stress relief analysis, or the deformation behaviour of the welding in connection with the prediction and control of dimensional changes. In such cases, a broader temperature distribution with subsequent elasto-plastic analysis is monitored using software such as Ansys [51], MSC. Marc or Sysweld [52].

The basic strength of the resulting fusion welded joint can be evaluated from two main points of view – shear stress and tensile stress [53–55]. The stress on joints from bending or torsion in the case of a multi-joint system is essentially always transformed into two of the above-mentioned fundamental stresses.

In the case of shear stress, the resulting stress is transmitted between the tab and the slot by the contact surfaces and partly by the weld. The joint strength is then defined by the shear strength of the tab neck τ_{maxT}, which is calculated from the relationship

$$\tau_{maxT} \geq \frac{F_s}{a \cdot b_n} \tag{4}$$

where F_s is the shear force and a, b_n represent the rectangular dimensions of the neck.

When tensile stress is applied to the joint where the tab is pulled out of the slot, the resulting strength is defined by a lower value of tensile strength of the weld or tensile strength of the neck of the tab. The tensile strength σ_{maxT} for the neck area of the tab is given by the relationship

$$\sigma_{maxT} \geq \frac{F}{a \cdot b_n}. \tag{5}$$

The tensile strength σ_{maxS} for the plug weld is then calculated from the equation

$$\sigma_{maxS} \geq \frac{F \cdot \alpha}{g \cdot h} \tag{6}$$

where F is the loading force, α is the factor of weld joint and the parameters g, h represent the rectangular dimensions of the slot. The value of the tensile coefficient of the weld is not generally defined for the case of welding and the method of stress and it is necessary to determine it based on experiments.

In practice, in most cases, it is necessary to assess the proposed tab and slot welded frame construction in particular from the point of view of the resulting rigidity [56–58], which is given by the particular design solution. It is advisable to use FEM for the calculation and possible subsequent optimization.

4. Experimental and numerical evaluation of the method

4.1. Laboratory experiments

To assess the mechanical properties and rigidity values of steel frame constructions under static stress by simple bending, five basic test samples were proposed. A standard structural steel with guaranteed weldability (S235JRG1/Fe360B) was chosen as the default material of the samples. It is the standard steel for common profiles as well as for cut metal sheets.

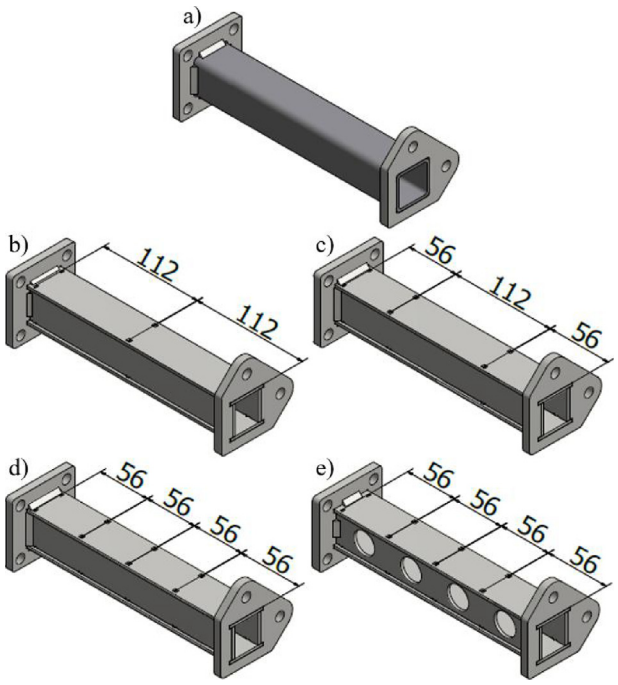

Fig. 4. Models of test samples – a) reference pattern (square tube), b) 3-joints, c) 4-joints, d) 5-joints, e) 5-joints with shape relief.

The reference sample was made from a common profile – a square tube (Fig. 4a). The other four samples were made by the tab and slot plug welded method, the difference being in the number of joints. The number of joints along the edge of the selected sample was three, four and five, as illustrated in Fig. 4b–d. Furthermore, the 5-joints sample had shape relief on the side panels of the structure (Fig. 4e).

Steel-welded test samples consisted of a body and two end flanges. The design allowed exact positioning of the sample in the selected direction of testing (0°, 90°). The body of the samples was composed of four 3-mm thick perpendicular plates, with the exception being the reference sample, which was a seamless square tube with a wall thickness of 3 mm. In each case, the sample flanges were fixed to the body by a fillet weld. The length of the test samples was 250 mm.

The samples were subjected to non-destructive tests (Fig. 5), i.e. the yield strength was not exceeded. The Lloyd Instruments type LR50K Plus laboratory press, equipped with a special, extremely rigid experimental sample fixation kit, was used for the tests. Each test sample was loaded with a 250 N initial force, with each additional measurement incremented by an additional 250 N, up to 1500 N. The upper limit was determined by numerical simulation of the reference sample. The speed of the crossbeam was set to 0.01 mm/s. After each measurement, the sample was visually inspected for plastic deformation, welding failure or crack propagation due to material defect. From a statistical point of view, each measurement was performed three times to guarantee the credibility and accuracy of the measurement. After completion of the entire measurement series, the sample was rotated by 90° and the entire loading cycle was repeated.

4.2. Numerical simulation

Numerical simulation was performed in an Autodesk Inventor design simulation environment. The final element model had a net-

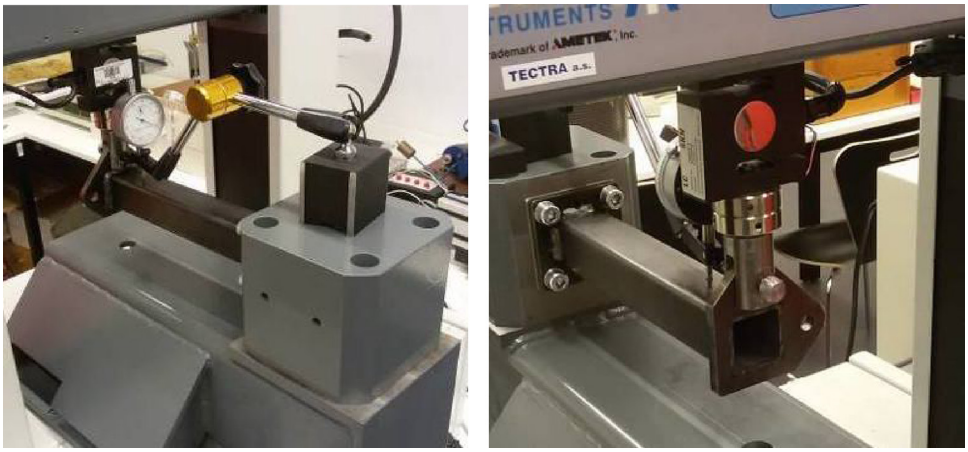

Fig. 5. Laboratory workplace with a prepared sample.

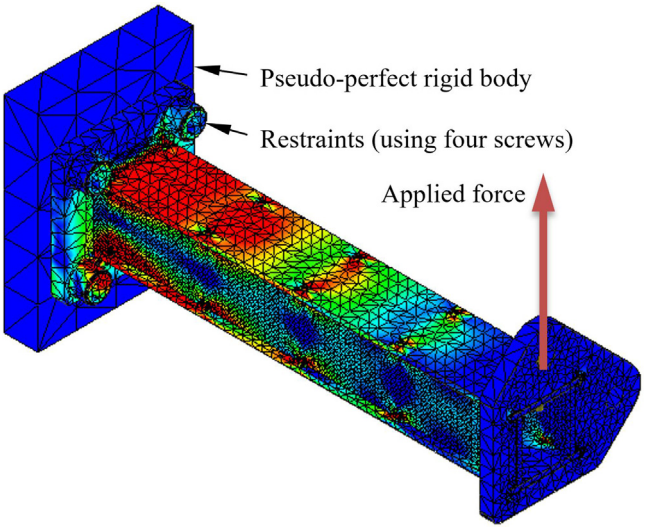

Fig. 6. Example of an adjusted FEM model of a test sample.

work of tetrahedra. Linear structural static analysis was performed based on the global equilibrium equation

$$\boldsymbol{R} = \boldsymbol{K} \cdot \boldsymbol{U} \tag{7}$$

where $\boldsymbol{R}$ is global loading matrix, $\boldsymbol{K}$ is global rigidity matrix and $\boldsymbol{U}$ is global displacement matrix [59,60].

The model (Fig. 6) was thoroughly adjusted in relation to the experimental results, with particular emphasis on the definition of boundary conditions, including the removal of the respective number of degrees of freedom, the definition of the individual contact points (areas) and, last but not least, the definition of the size of the weld joints. For a definition of the contact faces, the initial model was left to the default setting of the simulation generator, where the fixed contact was pre-set in all contact surfaces. Furthermore, a more accurate model with a manual contact surface setting was tested only on the areas of the joints, which correspond more closely to the real situation. The contact was assumed in a single contact area in the given direction for each joint. However, this manual procedure is relatively lengthy, which in the case of large assemblies greatly prolongs the preparation time of the simulation.

The resulting structure was evaluated mainly in terms of rigidity, i.e. the maximum deflection at the chosen load at the yield strength level, or more precisely slightly below the given value. In this area, in conformity with the tensile diagram of steel, the course of increasing stress on the reshaping has a linear character. It is obvious that the rigidity of the designed tab and slot plug welded construction can be reduced to a limited extent by decreasing the pitch joints or by increasing the number of joints at the appropriate distances. Furthermore, the rigidity will be determined by the frame design, i.e. the intensity and suitability of the rib placement. It will also depend on the presence, i.e. the position, shape and size of the shape relief.

The results of the numerical model were compared with the experimentally measured load characteristics of the tested samples. The comparison confirmed a very good match between the model and the course obtained by the experimental method for the entire area of loading. For a comparison of all of the tested samples, the maximum deflections obtained by the laboratory measurements and the finite-element model with the same loading force of 1500 N are shown in Table 1. The deflection of the reference sample was approximately 0.6 mm at a maximum load. Compared to the most ridged tab and slot test sample (5-joints sample), the maximum deflection compared to the reference sample was only 3%. Therefore, a 50–60 mm pitch of the joints can be considered as being sufficient for the given design case. Conversely, the 5-joints pattern relief showed a marked drop in rigidity, resulting in a deflection of up to 2× the level of the non-lightweight sample. In the 0° direction, the rigidity was greater than in the 90° direction, which was due to the quadratic momentum of the cross-section of the beams with the overlapping plate containing the slots.

5. Joint optimization

The technological conditions were formulated based on partial knowledge of the ongoing physical processes, in order to achieve the optimal results in terms of a rigid and solid joint. Emphasis was not placed on a theoretical evaluation of the process, but on practical experimentally-documented results. Due to the above-mentioned reasons (see Chapter 3), the presented optimization of the shape of the joints is based on experimental research resulting from general experience in the field of welding.

The optimization was divided into two stages. In the first stage, experiments focused mainly on the main joint factor, which is the height of the tab. In the second, main phase, the partial factors of the optimized method were mapped in detail based on the acquired knowledge. The plugs were performed in all cases using the MAG (CO_2) method [61,62]. The samples were tested in two versions, a conventional version with an untreated weld and further in a design version, i.e. with a grinded weld. The tests were performed on a 3-mm thick aluminium alloy plate (EN AW-5754 H22/AlMg3/ASTM B 209) and on 2 mm thick stainless steel samples (1.4301/X5CrNi18-

Table 1
Measured and calculated values of displacement and rigidity of samples.

Sample		Reference	5-joints		5-joints with shape relief		4-joints		3-joints	
Orientation		0°	0°	90°	0°	90°	0°	90°	0°	90°
Displacement [mm]	Experiment	0.58	0.60	0.69	0.90	1.22	0.65	0.81	0.68	0.81
	FEM	0.55	0.56	0.59	0.90	1.05	0.60	0.70	0.68	0.80
Rigidity [N/mm]	Experiment	2586	2500	2174	1667	1230	2308	1852	2206	1852
	FEM	2727	2679	2542	1667	1429	2500	2140	2206	1875
Weight without flanges [kg]		0.83	0.86		0.76		0.86		0.86	
$\frac{\text{Weight}}{\text{Rigidity}} \times 10^{-4}[-]$	Experiment	3.20	3.40	3.95	4.55	6.17	3.72	4.64	3.89	4.64
	FEM	3.00	3.20	3.14	4.74	5.32	3.40	4.01	3.89	4.63

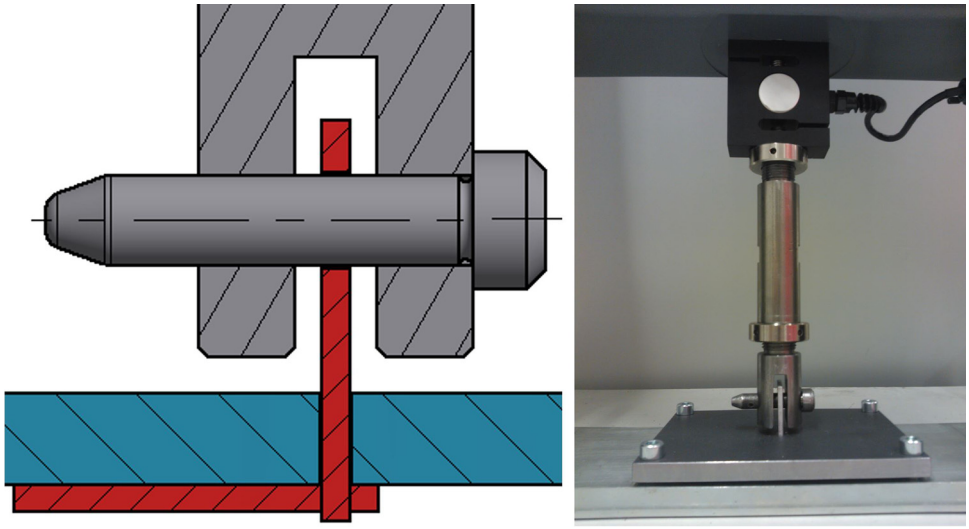

Fig. 7. Detail of the test workplace with the L-sample in place.

10/AISI 304). These values represent the normal lower limit of the thickness of the thin-walled profiles.

The experimental strength of the joints was tested by tensile tests, using the press that was used for the measurements presented in Chapter 4.1. The test samples were a welded L-profile with a single joint. Due to the placement of the parts and in particular the thermal deformation of the weldments, the samples were made in the form of longer (5-joints) pieces and then separated into single-joint samples. Part of the sample containing the slot was placed under a firmly mounted plate of the test preparation. The second section of the sample was inserted into the preparation with a tight cross-section (3.4 mm), which was connected using a pin and holes to a sliding crossbeam (Fig. 7). The crossbeam speed was set to the recommended test duration, i.e. approx. 60 s. For the aluminium alloy, it was set to 0.01 mm/s and for the stainless steel 0.02 mm/s. In most cases, a 5-kN force gauge with an accuracy of ±0.25% was used to measure load force, in a specific case given by a higher load, a 10-kN load gauge was used with an accuracy of ±0.25%.

For the aluminium alloy joints (Fig. 8a), the welding was primarily assumed, for technical reasons, to be a tab with an overlap over the slot. Specifically, test samples with tabs 1 mm ($c = d + 1$), 2 mm ($c = d + 2$) and 3 mm ($c = d + 3$) above the slot were tested. Furthermore, in order to verify the accepted assumptions, tabs with a 1 mm recession against the slot ($c = d - 1$) and at the level of the slot ($c = d$) were tested. In the case of the stainless steel (Fig. 8b), recessed joints were examined. Specifically, the tabs are recessed against the slot by 1 mm ($c = d - 1$), 0.5 mm ($c = d - 0.5$) and also at the level of the slot ($c = d$).

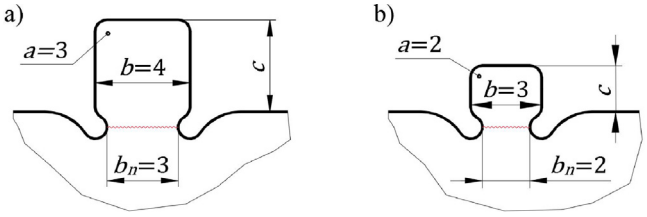

Fig. 8. Default dimensions of the tabs – a) aluminium alloy, b) stainless steel.

During the preparation of the samples it was found that, from the point of view of welding, the most advantageous in the case of aluminium alloys was a tab with a joint 1 mm ($c = d + 1$) or 2 mm ($c = d + 2$) above the level of the slot. If the tab is only at the level of the slot ($c = d$)), then it needs to be substantially heated, which leads to the burning of the edges of the plate containing the slot (see Fig. 9a). Conversely, if the tab is too far above the slot ($c = d + 3$), there is too much material at the welding point and there is not enough space for the added wire. From the point of view of the performed tensile test, it can be stated that the deformation of the joints in most cases occurred by the tab being pulled out of the slot, and the joint only broke in isolated cases in the area of the neck. In relation to the fact that the measured joint strength was similar in all cases, it can be concluded that the strength of the weld joint is generally equal to the strength of the neck. In the case of aluminium alloys, grinding the welds leads to a significant decrease in strength, as the weld is to a large extent above the level of the slot due to the protruding tab of the joint, i.e. in the resulting welded projection. Only in the case of the recessed tab or protrusion of the tab at the level of the slot, it is possible to perform the subsequent grinding

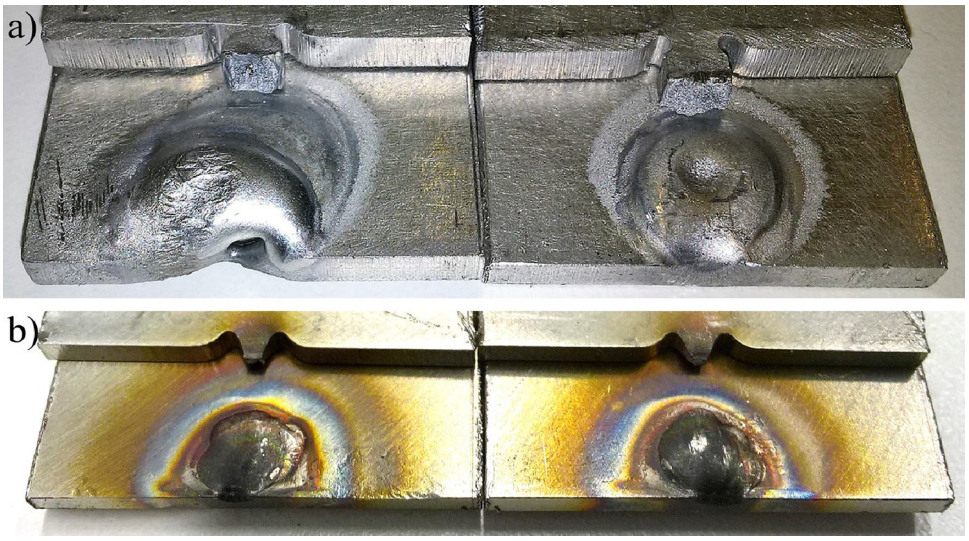

Fig. 9. Examples of deformation of sheet metal by welding – a) samples of aluminium alloy, b) samples of stainless steel.

without any significant impact on the resulting strength of the tab. However, this is inconsistent with the above-mentioned optimal welding technology.

For stainless steel joints, a tab at the level of the slot ($c = d$) or 0.5 mm below the level of the slot ($c = d - 0.5$) seem to be the optimal values from the point of view of welding. If the tab projection is too far below the level of the tab, then there is an undesirable burning of the edges (Fig. 9b). During the tensile tests, in all cases, the steel joints were destroyed at the point of the neck of the tabs, with a similar strength corresponding to the strength of the neck of the tab and corresponding to the theoretical calculations made based on relation (5). From this it can be concluded that the parameters of the joints, in the sense of inserting the tab against the slot, have no significant influence over the strength of the resulting joint within the tested range of dimensions, and it is therefore necessary to select them mainly with regard to the requirements of the welding technology.

5.1. Main experiments

The specific types of samples for the main experiments were designed in accordance with the findings of the examination stage. For the aluminium alloy samples (plate thickness $a = 3$ mm), both the starting length of the tab, i.e. $b = 4$ mm, and lengths of 5, 6 and 7 mm, were tested in detail. In addition, the influence of the size of the recesses, i.e. the necks of the tabs, was examined, mainly to assess the options and quality of the cut sheet production. The default narrowing value of the recess on each side was 0.5 mm, and the newly proposed value was 0.2 mm. This decrease was chosen for strength, i.e. the increase of the cross section of the neck of the tab, as well as aesthetic reasons, i.e. reduction of the holes remaining after the joint was connected to the interface of the parts.

The original value of the depth of the recess of 1.2 mm was changed to 0.4 and further to 0.2 mm (see Fig. 10a, samples A2, A0). The height of the tab above the slot was tested in the range of 0, 1 and 2 mm. For a height of 1 mm, the edges were also designed to be $1.5 \times 45^\circ$ and $2 \times 45^\circ$ (see Fig. 10a, samples 4 and 5). This was chosen to improve the joint welding while maintaining the optimal technological conditions of the welding.

In the case of the stainless steel samples (plate thickness $a = 2$ mm), both the original length of the joint, i.e. $b = 3$ mm, and the newly proposed lengths of 4 and 5 mm were tested (Fig. 10b). Another factor was the size of the recesses, which was the same as

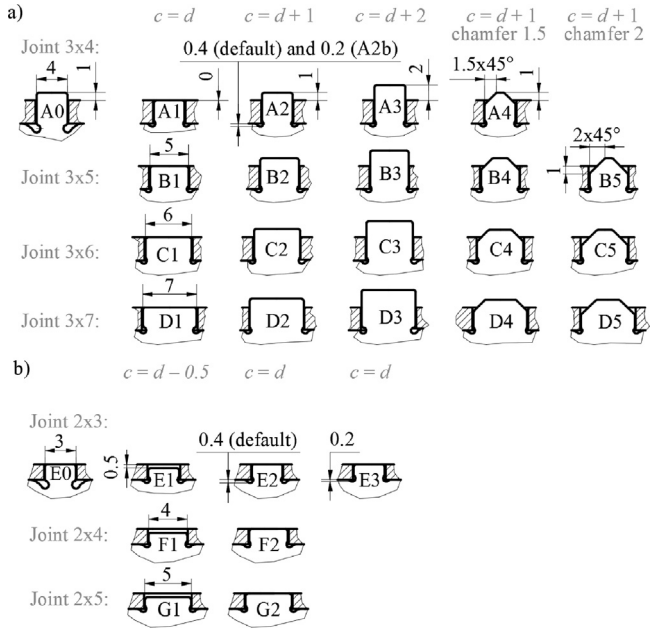

Fig. 10. Complete overview of tested sample types – a) aluminium alloy samples, b) stainless steel samples.

for the aluminium alloy samples, and also the dimensions, i.e. narrowing of the neck by 1 and 0.4 mm so the depth of visible recess was approximately 1.2, 0.4 and 0.2 mm. The height of the tab was tested at the same level as the slot and the recessed joint below the level of the slot i.e. 0.5 mm.

In the case of the aluminium alloy samples (Fig. 11a), increasing the aspect ratio of the tab, i.e. the length of the joint, was found to worsen the visual quality of the weld, since instead of the original pseudo-circular weld, a typical longitudinal caterpillar weld shape was formed. However, it is important to take this into account only if no additional grinding is performed. Reduction of the recess size (Fig. 11c) did not affect the quality of the joint, e.g. due to cutting burrs, which could affect the quality of the contraction of the slots. Of course, this cannot be fully generalized, since it depends on the cutting technology used and the particular cutting machine. However, both the laser and the water jet samples were tested with similar results. From an aesthetic point of view, the designer

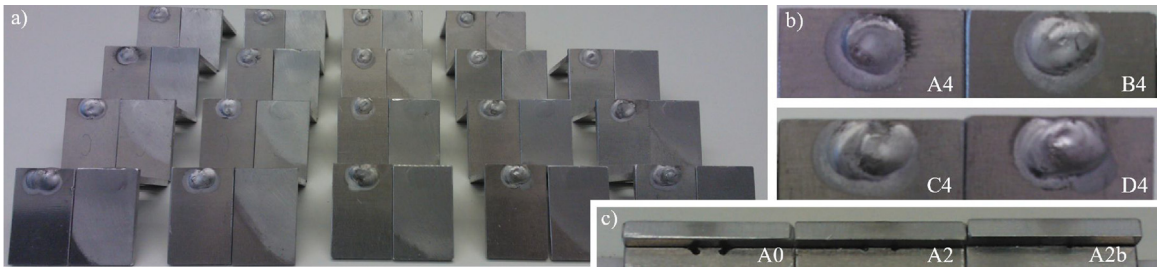

Fig. 11. Examples and close up of aluminium alloy samples – a) samples arranged in accordance with Fig. 10a (without A0), b) close up of untreated welds, c) close up of various different recesses.

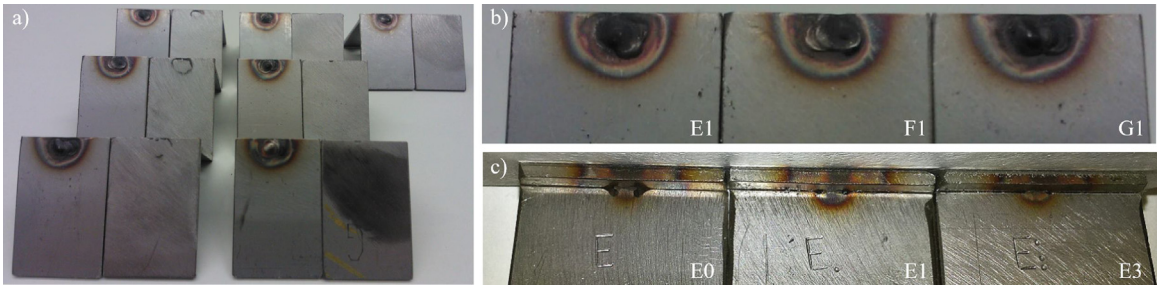

Fig. 12. Examples and close up of stainless steel samples – a) samples arranged in accordance with Fig. 10b (without E0), b) close up of untreated welds, c) close up of various different recesses.

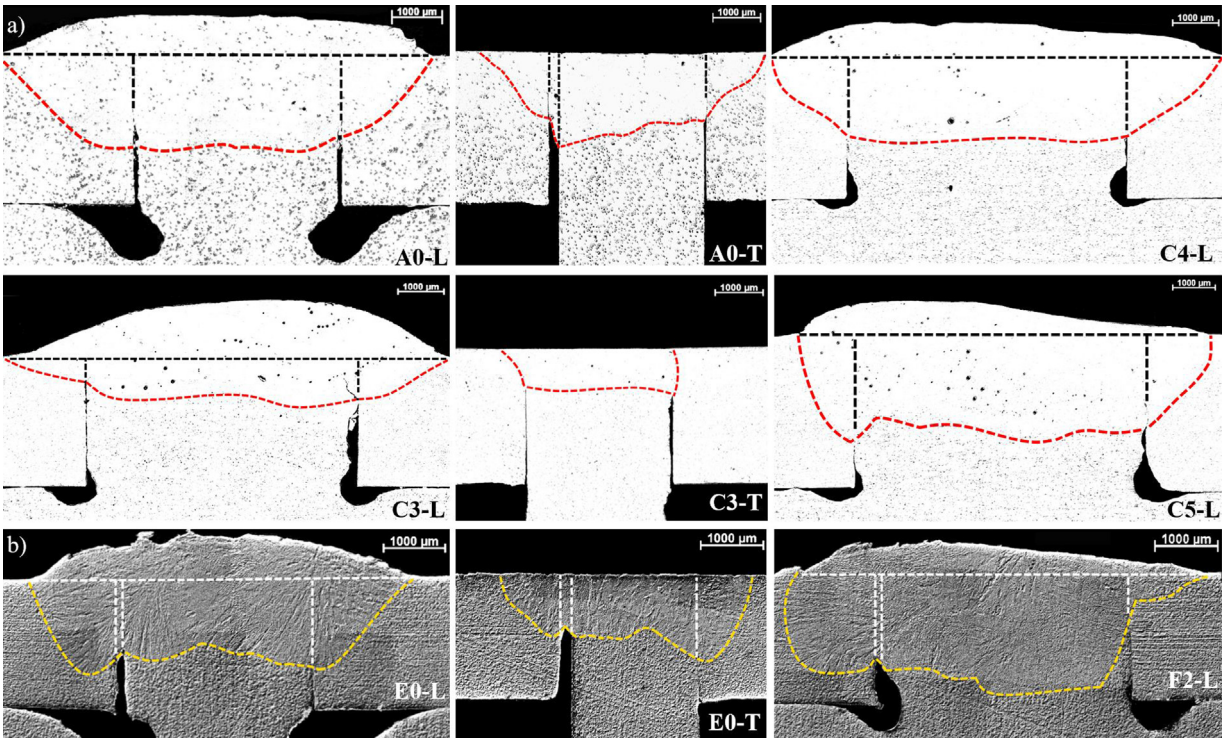

Fig. 13. Polished longitudinal (L) and transverse (T) cross sections of the tab and slot plug welded joints – a) aluminium alloy samples A0, C3, C4, and C5, b) stainless steel samples E0 and F2 (note: transverse samples are with grinded weld).

should assess whether they want to accept, emphasize, or disguise the recesses. The stainless steel samples (Fig. 12a) can be evaluated similarly to aluminium alloy samples. In the case of the longer joints, the weld is again a caterpillar shape, but the difference is not as noticeable for the given material (Fig. 12b), due in particular to the smallness of the weld. The recesses can be evaluated the same as for aluminium alloy samples, i.e. a reduction in the size of recess does not affect the quality of the joint (Fig. 12c). It is necessary to emphasize that one of the major factors influencing both the strength and the aesthetics of the joint, is the quality of the weld. This depends on the experience of the welder, both in terms of manual skills and also in the setting of the technological parameters of the welding aggregate. Microscopic images of the aluminium alloy and steel samples showing the shape of the longitudinal and transverse cross section of the tab and slot plug welded joint are included in Fig. 13., which illustrates the default joint (A0,

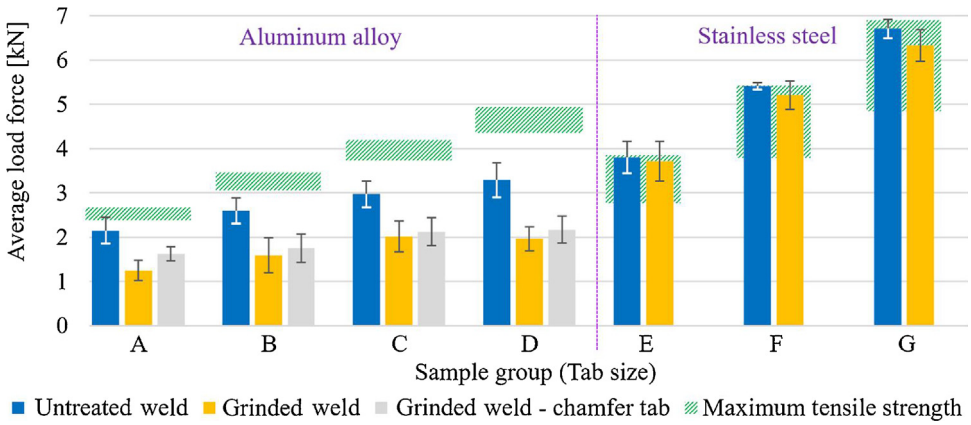

Fig. 14. Experimentally measured joint strength of aluminium alloy and stainless steel samples.

E0) and the optimal joints C4, C5 and F2. Images of the C3 sample are also shown, which show a smaller welding with respect to the large cant of the tab. Conversely, longitudinal cross sections of samples C4 and C5 show a deeper welding of the joints due to the chamfer of the tab. All of the steel samples have a similar welding in terms of the geometric characteristics of the respective joints. Approximate weld interfaces were found with use of image analysis method based on fractal geometry [63]. Dots on the aluminium alloy samples are related to small (or locally even large) pores. Using the electron microscope, it is obvious that apart from the light phases (Mg-based) there are numerous small pores in the aluminium emphasized by etchant. There are fewer of these pores in the weld as the welded metal has been remoulded and thus it is less porous.

A total of 21 aluminium alloy and 8 stainless steel samples were fabricated. Each type of sample was made in 10 designs, with 5 pieces being tested without welding treatment and the rest with a grinded weld. In total, 290 samples were tested during the main experiment. The results of the tensile tests for both of the tested materials are shown in the graph in Fig. 14. The graph includes the theoretical neck strengths calculated according to relationship (5). The samples were destroyed in two ways, either by breaking the tab at the narrowest point, i.e. the neck formed by the recesses, or tearing the tab from the weld, depending on the sample material used, the state of the weld (grinded or untreated), the cross-section of the joint or the length of the tab. The limit strength of the neck of the tab is easily calculated using relationship (5). In the case of tearing the tab from the slot, the resulting strength is given by relationship (6); however, the real value is difficult to determine because each weld is individual, i.e. its strength is determined by the specific production conditions in relation to the welder. This uncertainty must cover the tensile coefficient of the weld. In the case of the aluminium alloy, all of the samples were destroyed by tearing the tab from the weld. In the case of the stainless steel joints, destruction occurred in the neck area of the tab in most cases. Its cross-sections are therefore crucial, especially in the case of pseudo-square cross-sections. The reduction of the recess in relation to the tensile strength of the joint is insignificant in the case of the aluminium alloy samples. However, it is advisable not to raise the recesses above the initial limit, i.e. a 0.5-mm narrowing on each side. For the stainless steel joints, the recesses should be as small as possible from the point of view of strength, as the significance of the size of the recess decreases with an increasing length of the tab.

During the statistical evaluation of the results, the influence of the height of the tabs on the strength of the untreated weld joint was not demonstrated within the examined parameters for either of the tested materials. This is largely due to the variance of the measured values of the individual welds. Hence, it was possible to include all of the untreated samples from a single size (tab length) into one group. In the case of grinded welds, most of the aluminium alloy samples showed a significant reduction in strength. A statistically significant difference compared to the average was only demonstrated in the case of samples with bevelled tab edges, where the decrease in strength was reduced by an average of approximately 25%. This confirms the assumption that bevelling the edges of the tab can lead to a deeper joint welding, which remains even after the cap weld has been ground away (see Fig. 13). For stainless steel, the grinding effect was only observed on the G samples and especially on the G2 samples, where $c = d$. In this case, half of the untreated welds were destroyed by tearing the tabs from the welds, but all of the grinded welds were destroyed. However, it is necessary to emphasize that even in the case of the most significant difference between the strength of the grinded and untreated welds, the difference was only 5%.

The experiments generally confirmed that cross sections that were examined with different tab lengths had the most significant impact on joint strength. In the case of stainless steel, where destruction occurred particularly in the area of the tab, the joint strength increased linearly, in full consistency with the theoretical strength, even though it was around its upper limit. A moderate (5%) deviation from the norm was only observed in the above-mentioned case of the grinded samples (G2). For the aluminium alloy samples, where the joint was destroyed in the area of the weld, the joint strength also increased linearly with the cross section, but compared to the increase in the theoretical strength of the neck of the tab, it was only with a 60% intensity. The measured values for untreated welds ranged from 90% up to 75% of the lower tensile strength for the longest tab. For grinded welds, a further increase in strength was no longer observed between samples C and D. After grinding, the samples of length C can be considered as limit samples. The strength of the joint (omitting sample D) 60% for the shortest tabs (group A) and almost 70% for the longest tabs (group C) in relation to the untreated welds.

5.2. Numerical stress analysis of welded joints

The basic principle of the presented method creates a positive reinforcement effect on the frame construction. During welding, the thermal stresses on the melt pool creates pressure through thermal expansion, which attracts the tab to the slot. This effect is demonstrated here using a simplified model numerically simulating the joint stress analysis. Welding analysis in MSC.Marc software [64] was used during the simulation.

Computer simulation of the welding process is a relatively complicated mathematical task, which is parameterized by a range of specific boundary conditions. The parameters in the boundary con-

ditions of the weld flux, weld path and also the weld fill can be defined in the MSC.Marc software, and can be combined by selecting one of the following two approaches:

- Thermal boundary conditions in the area of the weld are characterized by a distributed heat flux, which can be applied to both the base and the additional material. In this case, it is not possible to define the temperatures of the calculation elements of the additional material.
- The second alternative is to define the temperatures at nodal points on the calculation elements of the additional material, whereby the heat flux can no longer be considered.

It can generally be assumed that the heat sources during the welding are described by a Gaussian distribution of the power density in the area [65,66]. In the simplest case, the welding heat flux is defined as a disk on the respective surface. In volumetric models, it is possible to use more complex geometric models, either a cylindrical or a double elliptical model. Pavelic's disc model of the welding heat source can be expressed as

$$q(x,y,z) = \frac{3Q}{\pi r^2} e^{-3x^2/r^2} e^{-3z^2/r^2} \tag{8}$$

where q is the heat flux rate per unit area, $Q = \eta \cdot U \cdot I$ is the applied power with the efficiency η, U is the voltage and I is the current. The parameter r is the radius of the disc, z is the local coordinate along the weld, and x is the coordinate on the perpendicular cut on the weld. This model can be used for both 2D (edges) and 3D geometric entities (surfaces of solids).

The more complex Goldak's double ellipsoidal model for specifying volume flow rates is given by the following two equations

$$q_f(x,y,z) = \frac{6\sqrt{3} f_f Q}{a_e b_e c_f \pi \sqrt{\pi}} e^{-3x^2/a_e^2} e^{-3y^2/b_e^2} e^{-3z^2/c_f^2} \tag{9}$$

$$q_r(x,y,z) = \frac{6\sqrt{3} f_r Q}{a_e b_e c_r \pi \sqrt{\pi}} e^{-3x^2/a_e^2} e^{-3y^2/b_e^2} e^{-3z^2/c_r^2} \tag{10}$$

where q_f and q_r are the heat flux rates per unit volume on the front and rear of the melt pool, a_e is the weld width along the x-axis, b_e is the weld depth along the y-axis, the coefficients c_f and c_r are the forward and rear lengths of the melt pool along the weld along the z-axis and define the dimensionless factors f_f and f_r such that

$$f_f = \frac{2}{1 + c_r/c_f}, f_r = \frac{2}{1 + c_f/c_r}. \tag{11}$$

The geometry of the double ellipsoidal model with the main parameters in relation to the local coordinate system is shown in Fig. 15. The heat fluxes given by the Eqs. (8)–(10) can be modified

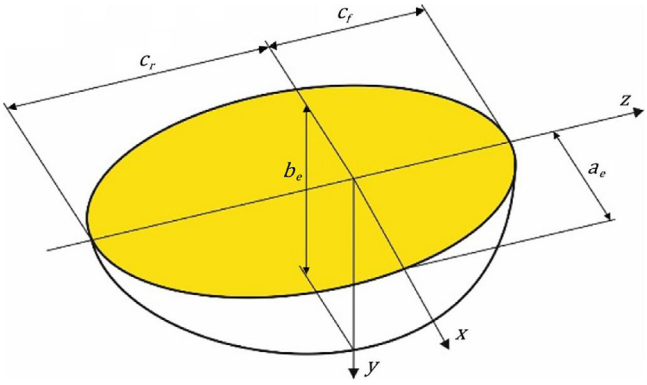

Fig. 15. Double ellipsoidal model of the weld.

by the scaling factor s, which, in particular for 2D solved problems, ensures an optimal conversion while respecting the thickness of the model t with regard to the applied power Q, whereby

$$s \iint q(x,y,0) t dx dy = Q \tag{12}$$

where $s = \sqrt{\frac{\pi}{3}} \frac{r}{t}$ or $s = \sqrt{\frac{\pi}{3}} \frac{(c_r + c_f)}{2t}$.

A simple computer model of an individual optimized tab and slot system was created respecting the geometry of the tested stainless steel samples, based on the theoretical assumptions and the previously mentioned possibilities of parameterizing of the welding process. The power was assumed to be approximately 2000 W with a 70% efficiency and welding speed of 2.5 mm/s along the weld path defined on the top of the tab. Mechanical and thermal material constants such as modulus of elasticity, Poisson's constant, thermal expansion, specific heat, and thermal conductivity were entered as a function of temperature. Latent heat was determined by the temperature of the solid and the liquid. The material model was also extended to respect the plasticity defined by the yield stress.

Despite the fact that the power of the welding aggregate and the temperatures were not precisely monitored during the welding of the experimental samples, the obtained simulation results can be considered to be very representative, as can be seen from the distribution of the stress and temperature fields in the area of the joint in Figs. 16–18 which correspond to the tested samples and confirm the development of contact stress between the contact surfaces of the connected parts due to thermal expansion.

Given that at the end of the welding process the average temperature of the tab is higher than that of the slot (Fig. 16), it is realistic to expect that after temperature equalization, the stress

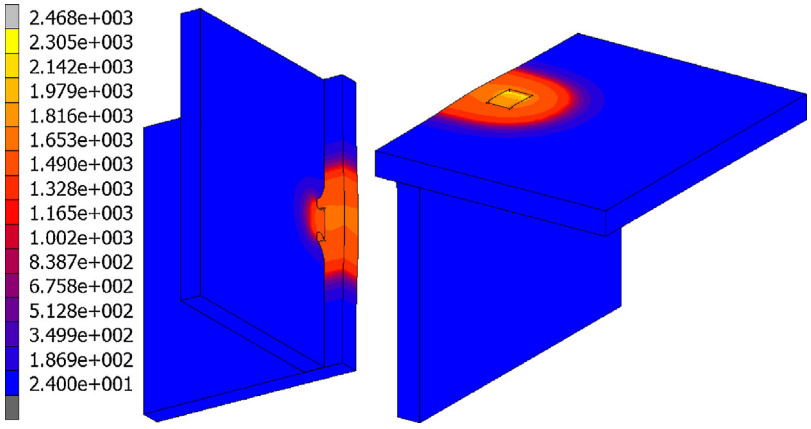

Fig. 16. Temperature field [°C] just after welding.

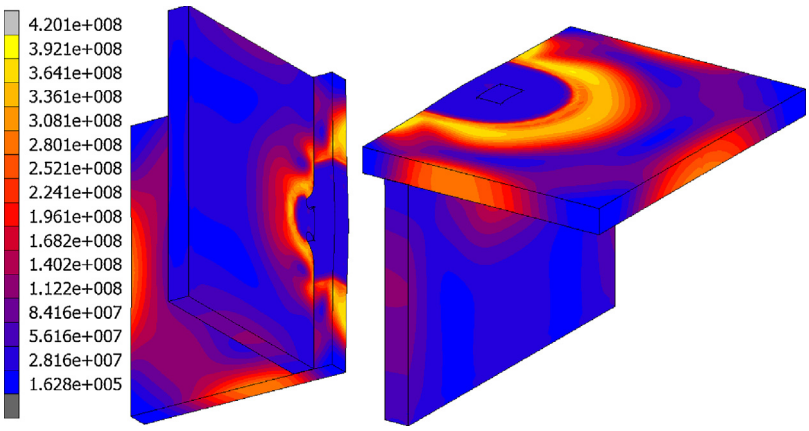

Fig. 17. Equivalent stress [Pa] just after welding.

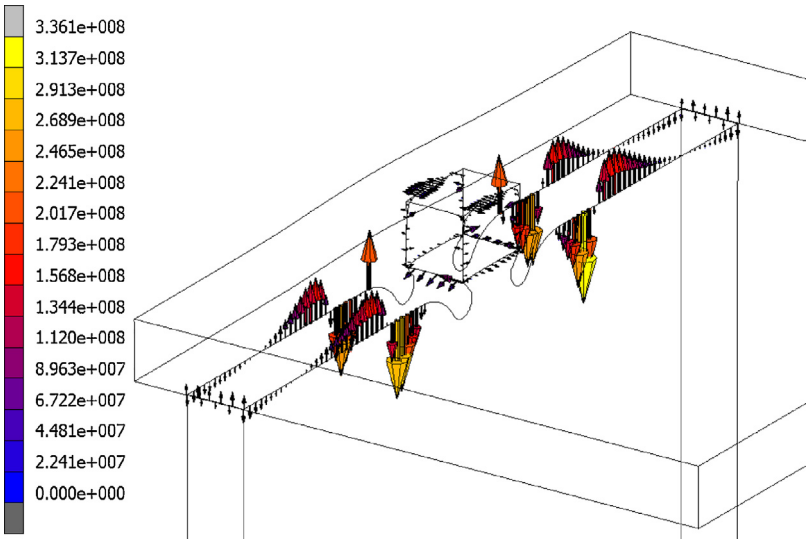

Fig. 18. Contact stress [Pa] just after welding.

will increase in the contact surface of the joint, whose rigidity will naturally increase due to thermal expansion.

6. Discussion and implemented applications

The result of the presented research is both the obtained technological knowledge about welding and the findings from the strength tests. The recommendations made must take into account both factors, depending on the specific application of the tab and slot plug welded construction in relation to the strength and weight requirements as well as the design. The findings are divided taking into account the studied materials – aluminium alloy and stainless steel. The results of the stainless steel can be generalized, i.e. applied to conventional structural steel. One of the most important factors influencing the strength of the joint as well as the aesthetics is the weld quality, which in turn depends on the experience of the welder, both in terms of their manual skills and in the setting of the technological parameters of the welding aggregate. Failure to follow the optimization criteria listed below may result in unnecessary degradation of the frame strength and in particular in manufacturing problems, such as melting edges.

For stainless steel, the joint strength was given by the strength of the neck of the tab, which was destroyed. The tensile strength was determined by relation (5) and the shear strength by Eq. (4). The choice of the joint parameters in terms of the tab recessed against the slot does not have a significant effect on the strength of the resulting joint within the tested dimensional range, and should therefore be selected with respect to the requirements of the welding technology, i.e. 0–0.5 mm from the level to the slot. In the case of requirements on the welding, it is better to incline the tab to the slot (value 0), since this does not display any residual craters after grinding. To increase the strength, it is recommended to modify the shape of the joint projection by minimizing the constriction in the neck area. This constriction is given by the recesses to facilitate assembly with the slot, the holes of which may have burrs around the edges due to the related manufacturing technology. The recess must be reduced based on the particular workplace producing the welds. In terms of aesthetics, the designer should evaluate whether to keep or mask the recesses, which they succeed in reducing. The dominant factor affecting joint strength is its cross-section. From the point of view of strength, it is recommended to use 2×5 mm joints, which have an increase in strength of over 70% compared to the initial cross-section (2×3 mm). A further significant increase in the length of the tab is not desirable, in particular in view of the possible thermal deformation of the structure. The twice the length of the tab in relation to the thickness of the plate rule can be applied to all of the plate thicknesses. In the case of welding, however, from a design point of view it is appropriate to keep to a pseudo-square profile, which creates an aesthetic weld. Considering the generally

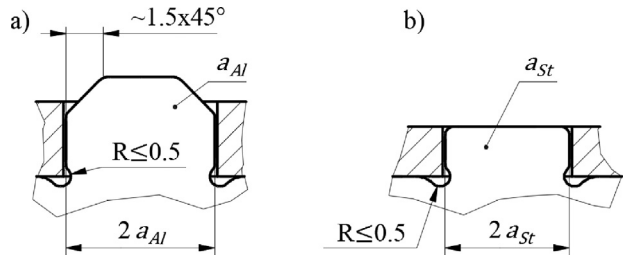

Fig. 19. Recommended form of the tabs for each material – a) aluminium alloy, b) steel.

relatively high strength of steel, it does not cause any substantial reduction in structural strength.

In the case of aluminium alloys, tabs of joints in the thin plate construction should be 1 mm above the level of the opposing piece from a technological point of view. It is also advisable to use joining protrusions in the form of 1.5 to $2 \times 45^{\circ}$ bevelled corners, which allow the outer corners of the tabs to reach 0.5–1 mm below the slot. This ensures maximum joint strength even after grinding. However, it is necessary to bear in mind that the decrease of the strength of the optimized joints by grinding is approximately 30%. The resulting tensile strength of the untreated joint is determined according to relation (6), where it is necessary to apply the factor of weld joint of approximately 0.75. For pseudo-square cross-sections of the joints, generally stated factor of weld joint (0.85) could be applied. If the weld is grinded, then it is necessary to apply an additional grinded weld failure coefficient of a minimum of 1.3, preferably 1.5. The shear joint is usually checked in the area of the neck according to Eq. (4). The most important effect on the strength of the tab and slot plug welded joint is, as with steel, the cross-sectional size of the joint. For 3 mm thick plates, an approximately 6 mm long joint is recommended, where the joint strength increases by approximately 40% relative to the basic cross section (3×4 mm). In the case of grinded welds, the use of larger joint cross sections does not lead to a decrease in their aesthetic qualities, since the welds can be completely ground down. If the designer wants to keep the welds, it is better aesthetically to use pseudo-square cross sections that form a circular welding reinforcement. Based on experience, it is possible to state that for the optimal joint parameters, i.e. the characteristic overlap and bevel of the tab and the rule of twice the length of the tab in relation to the thickness, the maximum plate thickness should be approximately 8 mm, which corresponds to the usual design requirements. For a single thicker plate with a slot, where the mass volume is capable of locally absorbing a greater amount of energy from the welding process, it is possible to apply a common steel construction process, i.e., recessing the joint at the level of the slot without modifying the corners of the tab. This also applies when both the plates are thicker, but a pseudo-square cross section of the joint should be used as it is then easier from a technological point of view to make the plug or slot weld in the given larger dimensions. From the point of view of optimizing the size of the recesses, for a default value of 0.5, it is possible to select the shape of the neck of the tab purely in relation to the design, because the welding area is weaker.

Fig. 19 shows the recommended form of the optimized tabs for each of the examined materials. The strength of the resulting tab and slot plug welded structure is generally influenced by the above-presented parameters of the joints but also by the number, the spacing, of the joints. In this regard, a range of 30–100 mm is recommended in relation to a particular design case. When designing the optimum number of joints, it is necessary to take into account, among other things, the financial costs of their construction. FEM is recommended for checking and optimizing the frame strength. The accuracy of the simulation results is largely influenced by the accuracy of the boundary conditions of the task. When designing common, especially steel, frames, where a safety factor of two or more is applied, a simplified automated procedure can be applied that generates a contact on all interfaces. This means errors of up to 20% can be acceptable. When designing lightweight structures with an emphasis on saving as much material or weight as possible, or there are higher demands on the resulting precision, it is necessary to use a more accurate procedure when creating the simulation model with manually set contacts in the areas of the joints only. In this case, the procedure should be chosen based on the complexity of the design and the professional judgment of the designer.

In general, the main features of the given method can be summarized in the following points:

- It is possible to create both cheap structural steel frames for conventional equipment and lightweight, yet rigid aluminium alloy frames for specific applications.
- High shape precision of the resulting welded structure is achieved without the use of positioning devices where, unlike the application of continuous or intermittent fillet welds, there is no thermal deformation of the frame and therefore in most cases it is not necessary to perform complicated and costly additional machining of the functional surfaces.
- It is possible to easily apply relief and variability to the walls while maintaining the required rigidity of the frame.
- It is possible to create a relatively interesting industrial design of exposed frame constructions for which aesthetic value can be increased by grinding the welds.
- The exposed structure provides easy access to the final frame for example for cabling.

Another interesting challenge may be automating the method using welding robots. Successful implementation would allow application of the present method in mass production.

6.1. Examples of implemented applications

The knowledge gained from the tab and slot welded frame design optimization has been utilized by the authors in a range of design applications, which are briefly presented below. Emphasis was placed not only on the rigidity of the construction but also on the aesthetic appearance, which in some cases was supported by shape relief in the form of triangular geometric shapes. The material left between the triangles serves as a stiffening rib. All of the following structures are tested for long-term operation.

The first example (Fig. 20) is the prototype frame of a compact matting effector [67] of an industrial robot designed for the technological operation of glass matting. The frame is made of a 4-mm thick steel plate, with only the contact elements (flanges) being made of a thicker 6 mm plate. This frame has a high rigidity in relation to the minimum weight, due to the shape relief parts.

The next example is a retractable pin (Fig. 21), designed for the Škoda Auto a.s. plant in Kvasiny (Czechia), for the purpose of vehicle uniform positioning by RPS (Reference Point System) for subsequent front-end installation. The supporting part of the retractable pin is an outer frame consisting of a tab and slot plug welded structure with 5-mm thick steel plates and an 8-mm thick support plate. The design system was chosen with regard to the simplicity of production, the compactness of the equipment and the aesthetic qualities.

The third example is a specifically designed welded frame of a special ergometer for rehabilitation of the lower limbs, using torque control functions that can change the torque in a defined manner during rotation of the handle. Due to the separate drive system, the torque can be implemented asymmetrically, i.e. differently for each limb, depending on the extent and type of disability. The

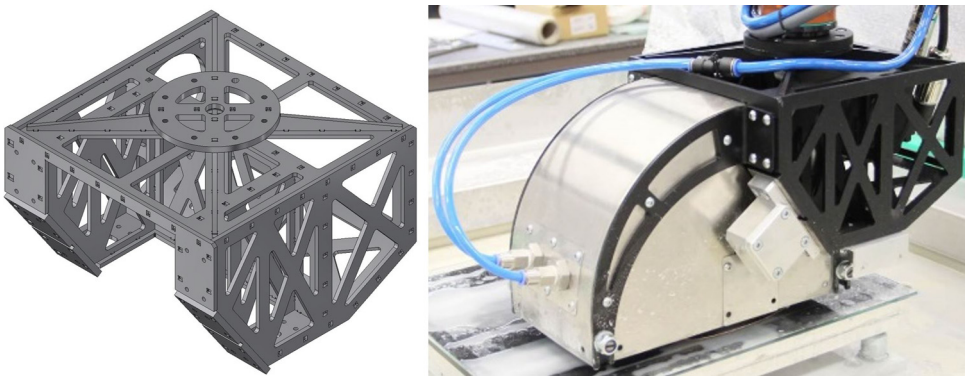

Fig. 20. Compact matting effector.

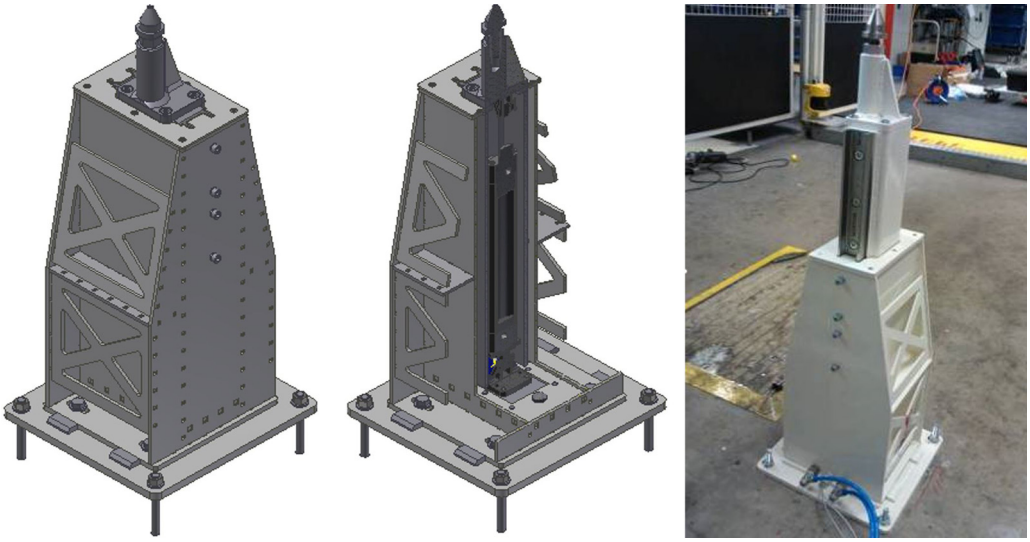

Fig. 21. Retractable RPS pin for vehicle positioning.

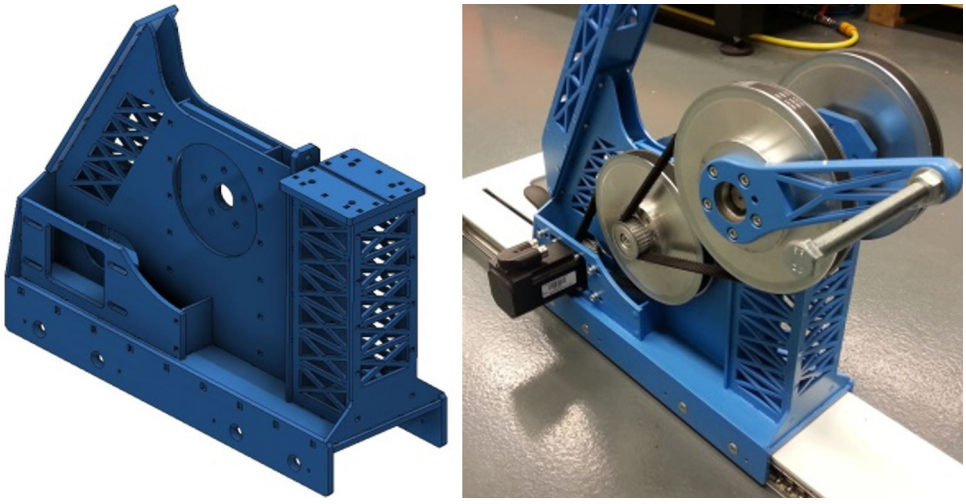

Fig. 22. Frame of an ergometer drive unit.

frame design (Fig. 22) minimizes the weight and cost of additional machining with sufficient shape precision. The initial thickness of the plate is 4 mm, with 6–8 mm plates used on stress points (areas).

The last example is the frame of a myotonometer (Fig. 23), which is a prototype of a second-generation medical device. The unique device evaluates muscle tension and determines the cause of muscle pain [68,69]. The aluminium alloy frame, made of 3 and 6 mm thick plates, was selected due to its low production costs and relatively high rigidity at a low weight for easy handling.

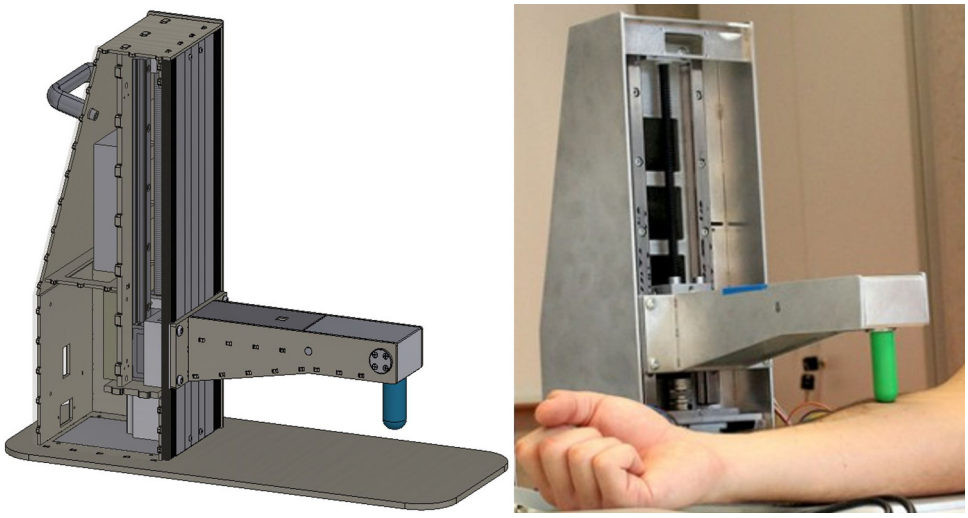

Fig. 23. Myotonometer.

7. Conclusion

The paper presents a method with high potential application for the production of plug welded structural frames. Both the experimental and the numerical simulation proved the interchangeability of the presented construction system with the common profile frame, provided that the specified rules were observed. In addition, the numerical simulation of stress fields in welded joints demonstrates the desirable effect of tightening. The main part of the paper describes the successful experimental optimization of joints in relation to used materials, i.e. steel and aluminium alloy. For both materials, the following conclusions are drawn:

(1) The dominant factor affecting joint strength is its cross-section. The twice the length rule, twice the tab length to the plate thickness, can be applied to all of the plate thicknesses. In the case that projections are not grinded after welding, however, from a design point of view it is appropriate to keep to a pseudo-square profile.
(2) The strength of the resulting structure is also influenced by joint spacing. Generally a range of 30–100 mm can be recommended.

Specifically for a steel construction, the following applies:

(3) The joint strength is given by the strength of the tab neck. Applied narrowing value of recesses is desirable to minimize. The height of the tab is suitable to choose aligned to the slot level. Grinding of the weld does not significantly influence the final strength.

In the case of aluminium alloy, it was found:

(4) The weakest area is the weld, the shape of the neck is not important and is primarily a matter of design. Tabs of joints should be 1 mm above the level of the opposing piece and with bevelled corners of 1.5–2 × 45°. The decrease of the strength of the optimized joints by grinding is approximately 30%.
(5) Using a single thicker plate (above 8 mm) with a slot makes it possible to apply a common steel construction process. When both the plates are thicker, it is desirable to use a pseudo-square cross section of the joint.

Acknowledgements

The results were obtained with co-funding from the project LO1201 financed by Ministry of Education Youth and Sports of the Czech Republic, as part of the targeted support from the programme entitled National Sustainability Programme I.

References

[1] Schubert E, Klassen M, Zerner I, Walz C, Sepold G. Light-weight structures produced by laser beam joining for future applications in automobile and aerospace industry. J Mater Process Technol 2001;115:2–8, http://dx.doi.org/10.1016/S0924-0136(01)00756-7.
[2] Tempelman E. Chapter 18 – lightweight materials, lightweight design? In: Materials Experience. Boston: Butterworth-Heinemann; 2014, http://dx.doi.org/10.1016/B978-0-08-099359-1.00018-7.
[3] Leyens Ch. In: Peters M, editor. Titanium and Titanium Alloys: Fundamentals and Applications. Weinheim: Wiley-VCH; 2005., http://dx.doi.org/10.1002/3527602119.
[4] Gottero M, Poidomani G, Tavera S, Sacchi E, Genbeltzu GA, et al. Development of light-weight multifunctional structures. In: SAE Technical Paper 2007-01-3130; 2007, http://dx.doi.org/10.4271/2007-01-3130.
[5] Belvin W, Watson J, Singhal S. Structural Concepts and Materials for Lunar Exploration Habitats, Space 2006. AIAA SPACE Forum; 2006, http://dx.doi.org/10.2514/6.2006-7338.
[6] Immarigeon J-P, Holt RT, Koul AK, Zhao L, Wallace W, Beddoes JC. Lightweight materials for aircraft applications, 35; 1995. p. 41–67, http://dx.doi.org/10.1016/1044-5803(95)00066-6.
[7] Njuguna J, editor. Lightweight Composite Structures in Transport: Design, Manufacturing, Analysis and Performance. UK: Elsevier Science Technology; 2016. ISBN: 978-1782423256.
[8] Prasad NE, Wanhill RJH, editors. Aerospace Materials and Material Technologies. Singapore: Springer; 2017., http://dx.doi.org/10.1007/978-981-10-2143-5.
[9] Negrelli V. From earth to heaven: how professional 3D Printing and Windform® GT material helped in the construction of drone and medical devices. Reinf Plast 2016;61:179–83, http://dx.doi.org/10.1016/j.repl.2016.08.001.
[10] Louisiana Tech developing improved carbon fiber drones. Reinf Plast 2015;59:258, http://dx.doi.org/10.1016/j.repl.2015.10.016.
[11] Elber W, Gunther Ch. What experience gained in the aerospace industry might be useful when using new materials in the Automotive industry, 1235. VDI-Berichte; 1995. p. 1–6.
[12] Claus L, Weitzel S. Self-tapping fasteners for lightweight designs. In: SAE Technical Paper 2014-01-0785; 2014, http://dx.doi.org/10.4271/2014-01-0785.
[13] Cui X, Zhang H, Wang S, Zhang L, Ko J. Design of lightweight multi-material automotive bodies using new material performance indices of thin-walled beams for the material selection with crashworthiness consideration. Mater Des 2011;32:815–21, http://dx.doi.org/10.1016/j.matdes.2010.07.018.
[14] Sepold G, Schubert E, Franz T, Klassen M. Laserstrahlschweißen von leichtbaukonstruktionen. DVS Berichte 1997;187:65–9.
[15] Witik RA, Payet J, Michaud V, Ludwig Ch, Månson J-AE. Assessing the life cycle costs and environmental performance of lightweight materials in automobile applications. Compos Part A 2011;42:1694–709.

[16] Hagedorn G. The power of sheet metal design: small changes cut production costs dramatically. Fabricator 2011;3 http://www.thefabricator.com/article/shopmanagement/the-power-of-sheet-metal-design.

[17] Shina SG. Principles of Design for Manufacturing, In Concurrent Engineering and Design for Manufacture of Electronics Products. US: Springer; 1991. p. 48–67, http://dx.doi.org/10.1007/978-1-4684-6518-1_3.

[18] Ackermann M, Šafka J, Zelený P, Lachman M, Keller P. Properties of models produced by direct selective laser melting technology. Appl Mech Mater 2014;693:231–6, http://dx.doi.org/10.4028/www.scientific.net/AMM.693.231.

[19] Lu L, Sharf A, Zhao H, Wei Y, Fan Q, Chen X, et al. Build-to-last: strength to weight 3D printed objects. ACM Trans Graph 2014;33:1–10, http://dx.doi.org/10.1145/2601097.2601168.

[20] Mainka H, Täger O, Körner E, Hilfert L, Busse S, Edelmann FT, et al. Lignin – an alternative precursor for sustainable and cost-effective automotive carbon fiber. J Mater Res Technol 2015;4:283–96, http://dx.doi.org/10.1016/j.jmrt.2015.03.004.

[21] Solvay's carbon fiber grade used to make automotive component. Reinf Plast 2016;60:73–4, http://dx.doi.org/10.1016/j.repl.2016.02.044.

[22] Teti R. Machining of composite materials. CIRP Ann – Manuf Technol 2002;51:611–34, http://dx.doi.org/10.1016/S0007-8506(07)61703-X.

[23] Duboust N, Melis D, Pinna C, Ghadbeigi H, Collis A, Ayvar-Soberanis S, et al. Machining of carbon fibre: optical surface damage characterisation and tool wear study. Proc CIRP 2016;45:71–4, http://dx.doi.org/10.1016/j.procir.2016.02.170.

[24] Campbell FC. Lightweight Materials: Understanding the Basics. Ohio: ASM, International; 2012. ISBN: 978-1615038497.

[25] Ashby MF. Materials Selection in Mechanical Design. Oxford: Elsevier Butterworth-Heinemann; 2011, http://dx.doi.org/10.1016/j.compositesa.2011.07.024. ISBN: 978-1856176637.

[26] Kissell JR, Ferry RL. Aluminum Structures: A Guide to Their Specifications and Design. New York: J. Wiley; 2002. ISBN: 978-0471387701.

[27] Messler RW. Joining of materials and structures: From pragmatic process to enabling technology. Oxford: Elsevier Butterworth-Heinemann; 2004.

[28] Shuster JW. Structural steel fabrication practices. New York: McGraw-Hill; 1997. ISBN: 978-0070577701.

[29] Barnes TA, Pashby IR. Joining techniques for aluminium spaceframes used in automobiles: part I – solid and liquid phase welding. J Mater Proc Techol 2000;99:62–71, http://dx.doi.org/10.1016/S0924-0136(99)00367-2.

[30] Jones FD. Jig and Fixture Design. New York: Industrial Press; 1955. ISBN: 978-0831110383.

[31] Russell DC. Self-Fixturing Architecture, Theses from the Architecture Program, Paper 133. 2012: University of Nebraska-Lincoln; 2017 http://digitalcommons.unl.edu/archthesis/133.

[32] Li J, Hunt JF, Gong S, Cai Z. Improved fatigue performance for wood-based structural panels using slot and tab construction. Compos Part A 2016;82:235–42, http://dx.doi.org/10.1016/j.compositesa.2015.12.017.

[33] J. Cornu, Advanced Welding Systems: 1 Fundamentals of Fusion Welding Technology, Springer Berlin, ISBN: 978-3662110515.

[34] Mraz S. Methods for fastening sheet metal without fasteners. In: Machine Design; 2015 http://www.machinedesign.com/mechanical/methods-fastening-sheet-metal-without-fasteners.

[35] Gordon L. Caterpillar creates innovative technologies to boost welding performance. Weld Des 2004 http://weldingdesign.com/processes/welding-innovations.

[36] Felton SM, Tolley MT, Onal CD, Rus D, Wood RJ. Robot self-assembly by folding: a printed inchworm robot. In: IEEE International Conference on Robotics and Automation (ICRA). 2013. p. 277–82, http://dx.doi.org/10.1109/ICRA.2013.6630588.

[37] Deng D, Liang W, Murakawa H. Determination of welding deformation in fillet-welded joint by means of numerical simulation and comparison with experimental measurements. J Mater Proc Techol 2007;183:219–25, http://dx.doi.org/10.1016/j.jmatprotec.2006.10.013.

[38] Perić M, Tonković Z, Rodić A, Surjak M, Garašić I, Boras I, et al. Numerical analysis and experimental investigation of welding residual stresses and distortions in a T-joint fillet weld. Mater Des 2014;53:1052–63, http://dx.doi.org/10.1016/j.matdes.2013.08.011.

[39] Teng T-L, Fung C-P, Chang P-H, Yang W-C. Analysis of residual stresses and distortions in T-joint fillet welds. Int J Pressure Vessels Piping 2001;78:523–38, http://dx.doi.org/10.1016/S0308-0161(01)00074-6.

[40] Zheng HY, Han ZZ, Chen ZD, Chen WL, Yeo S. Quality and cost comparisons between laser and waterjet cutting. J Mater Proc Tech 1996;62:294–8, http://dx.doi.org/10.1016/S0924-0136(96)02423-5.

[41] Hlaváč LM, Hlaváčová IM, Gembalová L, Kaličinský J, Fabian S, Měšťánek J, et al. Experimental method for the investigation of the abrasive water jet cutting quality. J Mater Proc Tech 2009;209:6190–5, http://dx.doi.org/10.1016/j.jmatprotec.2009.04.011.

[42] Krajcarz D. Comparison metal water jet cutting with laser and plasma cutting. Proc Eng 2014;69:838–43, http://dx.doi.org/10.1016/j.proeng.2014.03.061.

[43] Cho D-W, Kiran DV, Na S-J. Analysis of molten pool behavior by flux-wall guided metal transfer in low-current submerged arc welding process. Int J Heat Mass Transf 2017;110:104–12, http://dx.doi.org/10.1016/j.ijheatmasstransfer.2017.02.060.

[44] Unnikrishnakurup S, Rouquette S, Soulié F, Fras G. Estimation of heat flux parameters during static gas tungsten arc welding spot under argon shielding. Int J Therm Sci 2017;114:205–12, http://dx.doi.org/10.1016/j.ijthermalsci.2016.12.008.

[45] Lancaster JF, editor. The physics of Welding, International Institute of Welding. Oxford: Pergamon; 1986. ISBN: 978-0-08-034076-0.

[46] Choo RTC, Szekely J, Westhoff RC. Modelling of high-current arcs with emphasis of free surface phenomena in the weld pool. J Weld 1990;69:346–61 https://app.aws.org/wj/supplement/WJ_1990_09_s346.pdf.

[47] Otto A, Schmidt M. Towards a universal numerical simulation model for laser material processing. Phys Proc 2010;5:35–46, http://dx.doi.org/10.1016/j.phpro.2010.08.120.

[48] Courtois M, Carin M, Le Masson P, Gaied S, Balabane M. A new approach to compute multi-reflections of laser beam in a keyhole for heat transfer and fluid flow modelling in laser welding. J Phys D Appl Phys 2013;46:505305, http://dx.doi.org/10.1088/0022-3727/46/50/505305.

[49] Lu SP, Dong WC, Li DZ, Li YY. Numerical simulation for welding pool and welding arc with variable active element and welding parameters. J Sci Technol Weld Join 2009;14:509–16, http://dx.doi.org/10.1179/136217109X441182.

[50] Cao Z, Yang Z, Chen XL. Three-Dimensional simulation of transient GMA weld pool with free surface. Weld J 2004;83:169–76 https://www.flow3d.com/wp-content/uploads/2014/08/Three-Dimensional-Simulation-of-Transient-GMA-Weld-Pool-with-Free-Surface.pdf.

[51] Koo BS. Simulation of Melt Penetration and Fluid Flow Behavior during Laser Welding, Dissertation. Bethlehem: Lehigh University; 2013 http://preserve.lehigh.edu/cgi/viewcontent.cgi?article=2319&context=etd.

[52] Xu JJ, Gilles P, Duan YG. Simulation and validation of welding residual stresses based on non-Linear mixed hardening model. Strain 2012;48:406–14, http://dx.doi.org/10.1111/j.1475-1305.2012.00836.x.

[53] Hicks J. Weld Joint Design. England: Abington Publishing; 1999. ISBN: 978-1855733862.

[54] The Procedure Handbook of Arc Welding. Cleveland: Lincoln Electric Co.; 1994. ISBN: 978-9994925827.

[55] Yeo RBG, Barber H. Welds and design for welding. In: Steel Designers' Manual. Oxford: Blackwell Science; 2005, http://dx.doi.org/10.1002/9780470775097.ch24.

[56] Ballio G, Mazzolani FM. Theory and design of steel structures. London: Chapman and Hall; 1983.

[57] Bansal RK. A Text Book of Strength of Materials. New Delhi: Laxmi Publications; 2010. ISBN: 978-8131808146.

[58] Masubuchi K. Analysis of Welded Structures: Residual Stresses, Distortion and Their Consequences. London: Pergamon Press; 1980. ISBN: 978-0080227146.

[59] MSC. Marc Volume A. Theory and User Information, MSC Software Corporation, 2014, Santa Ana, CA.

[60] Oñate E. Structural Analysis with the Finite Element Method. Springer; 2009, http://dx.doi.org/10.1007/978-1-4020-8733-2.

[61] Mathers G. The Welding of Aluminium and Its Alloys. Elsevier Woodhead Publishing; 2002. ISBN: 978-1855735675.

[62] Weman K. Welding Processes Handbook. Elsevier Woodhead Publishing; 2011. ISBN: 978-0857095107.

[63] Hotař V. Fractal geometry for industrial data evaluation. Comp Math Appl 2013;66:113–21, http://dx.doi.org/10.1016/j.camwa.2013.01.015.

[64] MSC. Marc Volume C: Program Input, MSC. Software Corporation, 2014, Santa Ana, CA.

[65] Goldak J, Chakravarti A, Bibby M. A new finite element model for welding heat sources. Metall Trans B 1984;15:299–305, http://dx.doi.org/10.1007/BF02667333.

[66] Chaboudez C, Clain S, Glardon R, Mari D, Rappaz J, Swierkosz M. Numerical modeling in induction heating for axisymmetric geometries. IEEE Trans Magn 1997;33:739–45, http://dx.doi.org/10.1109/20.560107.

[67] Novotný F, Horák M, Starý M. Abrasive cylindrical brush behaviour in surface processing. Int J Mach Tool Manuf 2017;118–119:61–72, http://dx.doi.org/10.1016/j.ijmachtools.2017.03.006.

[68] Šifta P, Süssová J. A new method for measuring stiffness of soft tissue. Int J Rehabil Res 2009;32:35–6. ISSN: 0342-5282.

[69] Kysela M, Kolář M. Myotonometer – device for measurements of viscoelastic characteristics of soft tissues. ELEKTRO 2016-11th Internat. Conf 2016:556–60. ISBN: 978-1467386982.